THE JOURNAL OF BIOLOGICAL CHEMISTRY VOL. 287, NO. 7, pp. 5102–5111, February 10, 2012

Inactivation of *arf-bp1* Induces p53 Activation and Diabetic Phenotypes in Mice*[S]

Received for publication, November 10, 2011, and in revised form, December 19, 2011 Published, JBC Papers in Press, December 20, 2011, DOI 10.1074/jbc.M111.322867

Ning Kon[‡], Jiayun Zhong[‡], Li Qiang[§], Domenico Accili[§], and Wei Gu[‡¶1]

From the [‡]Institute for Cancer Genetics, [§]Naomi Berrie Diabetes Center, Department of Medicine, and [¶]Department of Pathology and Cell Biology, Columbia University College of Physicians and Surgeons, New York, New York 10032

Background: ARF-BP1 is involved in Mdm2-independent p53 degradation.
Results: Inactivation of *arf-bp1* in mice resulted in p53 activation and embryonic lethality. Inactivation of *arf-bp1* in pancreatic β-cells resulted in diabetes, which was partially rescued by loss of p53.
Conclusion: p53 is critically regulated by ARF-BP1 *in vivo* and in β-cells.
Significance: ARF-BP1 is important for maintaining pancreatic β-cell homeostasis in aging mice.

It is well accepted that the Mdm2 ubiquitin ligase acts as a major factor in controlling p53 stability and activity *in vivo*. Although several E3 ligases have been reported to be involved in Mdm2-independent p53 degradation, the roles of these ligases in p53 regulation *in vivo* remain largely unknown. To elucidate the physiological role of the ubiquitin ligase ARF-BP1, we generated *arf-bp1* mutant mice. We found that inactivation of *arf-bp1* during embryonic development in mice resulted in p53 activation and embryonic lethality, but the mice with *arf-bp1* deletion specifically in the pancreatic β-cells (*arf-bp1*$^{FL/Y}$/*RIP-cre*) were viable and displayed no obvious abnormality after birth. Interestingly, these mice showed dramatic loss of β-cells as mice aged, and >50% of these mice died of severe diabetic symptoms before reaching 1 year of age. Notably, the diabetic phenotype of these mice was largely reversed by concomitant deletion of p53, and the life span of the mice was significantly extended (*p53*$^{LFL/FL}$/*arf-bp1*$^{FL/Y}$/*RIP-cre*). These findings underscore an important role of ARF-BP1 in maintaining β-cell homeostasis in aging mice and reveal that the stability of p53 is critically regulated by ARF-BP1 *in vivo*.

The p53 tumor suppressor acts as the major sensor for a regulatory circuit that monitors signaling pathways from diverse sources, including DNA damage, oncogenic events, ribosomal stress, and other abnormal cellular processes (1–4). Although p53 mutations have been documented in more than half of human tumors, defects in other key components of the p53 pathway are frequently observed in tumor cells that retain wild type p53. Thus, inactivation of p53 appears to be a common, if not universal, feature of human cancer. It is well accepted that Mdm2 plays a major part in the scope of inhibition of p53 activities in cancer cells. Mdm2, a RING finger oncoprotein, acts as a specific E3 ubiquitin ligase in p53 degradation. The critical role of Mdm2 in regulating p53 is best illustrated by studies carried out in mice where deletion of *p53* was shown to rescue completely the embryonic lethality caused by the loss of Mdm2 function (5–7). Although numerous studies validate the crucial role of Mdm2 in regulating p53 stability, p53 still undergoes proteasome-mediated degradation in Mdm2-null cells (8). Accumulating evidence indicates that Mdm2-independent mechanisms are also involved in tissue-specific and temporal control of the stability and function of p53 *in vivo*. Indeed, the recently discovered E3 ligases COP1 (9), Pirh2 (10), Arf-BP1 (11), and others have clearly been shown to contribute to the efficient control of p53 levels in tissue culture and in *in vitro* biochemical experiments. Additionally, USP4 inhibits p53 activity indirectly through regulation of ARF-BP1 (12). Thus, both Mdm2-dependent and Mdm2-independent mechanisms are required to tightly regulate p53 function *in vivo*.

ARF-BP1, also known as MULE/HectH9/HUWE1, was originally identified as a major binding protein associated with ARF tumor suppressor. The ARF tumor suppressor acts as a key sensor of hyperproliferative signals such as those emanating from the Ras and Myc oncoproteins (13). Numerous studies indicate that ARF suppresses aberrant cell growth in response to oncogene activation by activating the p53 pathway (14). The ARF induction of p53 appears to be mediated through Mdm2 because overexpressed ARF interacts directly with Mdm2 and inhibits its ability to promote p53 degradation (15). Interestingly, ARF also has tumor suppressor functions that do not depend on p53 or Mdm2. ARF-BP1 harbors a signature HECT (homolog to E6-AP C terminus) motif, and its ubiquitin ligase activity is inhibited in the presence of ARF. Notably, inactivation of ARF-BP1, but not Mdm2, suppresses the growth of p53-null cells in a manner reminiscent of ARF induction. Indeed, several recent studies showed that ARF-BP1 is capable of ubiquitinating several p53-independent targets, such as Mcl-1, *N*-Myc, and Cdc6, leading to diverse functions (16–21). Surprisingly, in p53 wild-type cells, ARF-BP1 inactivation serves to stabilize the p53 polypeptide and activates p53 function. We further show that ARF-BP1 directly binds and ubiquitinates p53 and that inactivation of endogenous ARF-BP1 is crucial for

* This work was supported, in whole or in part, by a National Institutes of Health grant from the NCI. This work was also supported by a grant from the Leukemia and Lymphoma Society (to W. G.) and by Diabetes Research Center Grant DK63608 (to D. A.).
[S] This article contains supplemental Fig. 1.
[1] Ellison Medical Foundation Senior Scholar in Aging. To whom correspondence should be addressed: Institute for Cancer Genetics, Dept. of Pathology and Cell Biology, Columbia University College of Physicians and Surgeons, 1130 St. Nicholas Ave., New York, NY 10032. Tel.: 212-851-5282; Fax: 212-851-5284; E-mail: wg8@columbia.edu.

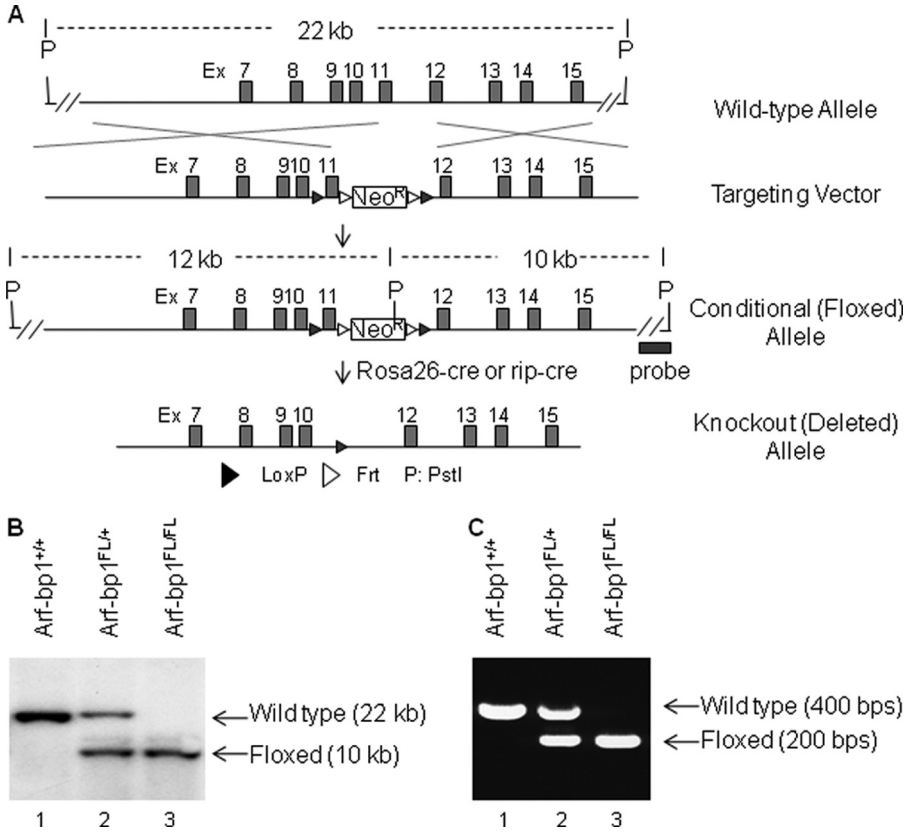

FIGURE 1. **Targeting scheme for generation of *arf-bp1* conditional knock-out mice.** *A*, gene targeting scheme of mouse *arf-bp1*. The wild-type allele represents the genomic region surrounding the exon 11, whereas *P* indicates restriction sites for PstI (wild-type allele). Targeting vector contains exon 11 with flanking loxP sites and 7-kb 5′ homology and 4 kb 3′ homology (targeting vector). After homologous recombination, the conditional knock-out allele is identified based on altered restriction fragments of PstI (conditional allele). Upon expression of rosa26-cre or RIP-cre, the conditional knock-out allele was converted to knock-out (exon 11-deleted) allele. *B*, genotyping by Southern blotting using genomic DNA digested by PstI. Hybridization with 3′ external probe detected a 22-kb band in wild-type mice (*arf-bp1*$^{+/+}$), and an additional 10-kb band for the floxed *arf-bp1* allele in heterozygote mice (*arf-bp1*$^{FL/+}$). Only the floxed band can be detected in *arf-bp1* conditional knock-out homozygote mice (*arf-bp1*$^{FL/FL}$ or *arf-bp1*$^{FL/Y}$). *C*, genotyping determined by PCR using mixed three primers to detect wild-type allele (400 bp) and the floxed allele (200 bp) simultaneously to identify wild-type mice, heterozygote mice, and homozygote mice.

ARF-mediated p53 stabilization in Mdm2-null cells (11). Together, these studies indicate that ARF-BP1 is a critical mediator of both the p53-independent and p53-dependent tumor suppressor functions of ARF. Nevertheless, it remains unclear whether ARF-BP1 is indeed required in regulating p53 *in vivo*, and the physiological role of ARF-BP1 also needs to be further elucidated.

To elucidate the physiological roles of ARF-BP1, we have generated *arf-bp1* conditional knock-out mice to study the effects of ARF-BP1 ablation on mouse development and on mouse pancreatic β-cell functions. Because p53 activation is difficult to detect in pancreatic β-cells, we speculate that p53 is potentially tightly controlled by multiple E3 ubiquitin ligases, including ARF-BP1. Moreover, studying ARF-BP1 in β-cells could potentially uncover p53-independent functions of ARF-BP1, if p53 were indeed greatly suppressed in β-cells. Deletion of *arf-bp1* during early embryonic development in mice resulted in embryonic lethality around embryonic day 14.5 (E14.5).[2] Furthermore, deletion of *arf-bp1* specifically in pancreatic β-cells caused dramatic loss of β-cells and development of age-dependent diabetes in mice. Notably, concomitant deletion of p53 effectively diminished the diabetic phenotype and also significantly elongated the life span of these *arf-bp1* mutant mice, suggesting an important role of ARF-BP1 in maintaining β-cell homeostasis through suppressing p53 functions. These results indicate ARF-BP1 as a critical regulator of β-cell homeostasis in aging mice and also suggest that p53 is a potential target in therapeutic treatment of diabetes.

EXPERIMENTAL PROCEDURES

Generation of arf-bp1 Conditional Knock-out Mice—To construct the *arf-bp1* gene targeting vector, a BAC clone (RP22-407A2) containing the 5′ portion of *arf-bp1* was screened from mouse the RP22 BAC genomic library (CHORI, Oakland, CA). We decided to delete exon 11 of *arf-bp1* (Ensembl), leading to a translational reading frameshift and loss of >90% of ARF-BP1 protein, including the HECT E3 ubiquitin ligase domain at the C terminus. The targeting vector was constructed by recombineering as described previously (22), which contained a 7-kb 5′ region of exon 11 and 4-kb 3′ region of exon 11 of *arf-bp1*. As indicated in the diagram (Fig. 1*A*), loxP sites were inserted in the introns flanking exon 11, to permit deletion of exon 11 upon expression of Cre recombinase. The targeting vector was linearized and electroporated into ES cells. After selection in the

[2] The abbreviations used are: E, embryonic day; Ad, adenovirus; GTT, glucose tolerance test; MEF, mouse embryonic fibroblast; *RIP-cre*, rat insulin promoter-controlled *cre*.

presence of G418, the targeted ES cell clones were identified by Southern blotting using PstI-digested ES cell genomic DNA and a 3′ probe, amplified with a 5′ primer of cctgataaattacctggagac and 3′ primer of aacagctaatggcagagggtt. The targeted ES cell clones were subsequently injected into blastocysts to generate chimera, from which the exon 11-floxed allele was transmitted through the germ line. Initially, genotyping was determined by Southern blotting (Fig. 1*B*). Subsequently, it was determined by PCR using primers of WT 5′ primer ctaatcacaggaagcggttacaag WT 3′ primer ctcctatagcaaagtaaaagtatag, and Neo primer gttattaggtggatccgtacgat to detect the wild-type allele and mutant allele simultaneously (Fig. 1*C*). The *arf-bp1* conditional knock-out mice were back-crossed to C57BL/6J to produce a congenic strain for the study of ARF-BP1 functions in β-cells. The *p53* conditional knock-out mice were kindly provided by Dr. Thomas Ludwig, Columbia University (23). Maintenance and experimental protocols using mice were approved by Institutional Animal Care and Use Committee (IACUC) of Columbia University.

Analysis of arf-bp1 Conventional Knock-out Mice—Breeding between *arf-bp1*$^{FL/+}$ female mice and *Rosa26-cre* homozygote male mice were set up to generate *arf-bp1* knock-out mice. The resulting offspring should have equal numbers of *arf-bp1*$^{+/+}$, *arf-bp1*$^{+/Y}$, *arf-bp1*$^{+/-}$, and *arf-bp1*$^{-/Y}$, among which *arf-bp1*$^{+/+}$ and *arf-bp1*$^{+/Y}$ represent wild-type embryos, *arf-bp1*$^{+/-}$ represents heterozygote embryos, and *arf-bp1*$^{-/Y}$ represents knock-out embryos. No viable *arf-bp1* knock-out mice were obtained postnatally, indicating that *arf-bp1* knock-out mice were embryonic lethal. Subsequently, phenotypic analysis was done using embryos collected from timed pregnancy at different stages of gestation. Embryos were fixed in PBS-buffered 4% paraformaldehyde overnight and embedded in paraffin. Serial 5-μm sagittal sections were collected and stained by hematoxylin and eosin according to standard procedures. The sections were also immunostained using antibodies against ARF-BP1 (ureb1; Bethyl), p53 (CM5; Novocastra), and Cleaved Caspase3 (Cell Signaling), followed by counterstaining using hematoxylin.

Histology and Immunohistochemical Analysis of Islets—Mouse pancreases were collected, fixed in 4% paraformaldehyde overnight, and embedded in paraffin. Sections of 5 μm were prepared and immunostained according to standard procedures, using antibodies against ARF-BP1 (Bethyl), insulin (Dako), and glucagon (Dako).

Determination of Blood Glucose and Insulin and Glucose Tolerance Test (GTT)—The *arf-bp1* conditional knock-out mice were back-crossed to C57BL/6J at least 6 times before crossing with transgenic *RIP-cre* (rat insulin promoter controlled *cre*) mice to generate *arf-bp1*$^{FL/Y}$*/RIP-cre* mice (24, 25). Because *arf-bp1* is located on the X chromosome, only the male mice (*arf-bp1*$^{FL/Y}$ and *arf-bp1*FL/Y$^{FL/Y}$*/RIP-cre*) were used in the subsequent study. The mice were maintained at a 12-h light/dark cycle. The fasting glucose levels and the fasting insulin levels were determined after the mice were fasted overnight (16 h). The fed glucose levels were measured using mice fed *at libitum*. The fed insulin levels were determined after mice were first fasted overnight and then fed *at libitum* for 4 h to maximize insulin secretion. Blood glucose was measured using blood from tail vein with OneTouch UltraMini glucometer (LifeScan; Johnson & Johnson). The blood insulin levels were determined using an Insulin ELISA kit (Millipore) according to the manual provided by the manufacturer. The GTT was done using mice fasted overnight before injecting 2 g of glucose/kg of body weight into the peritoneal cavity. Blood glucose levels were then determined at 15-, 30-, 60-, and 120-min time points after the glucose injection.

Deletion of arf-bp1 in Mouse Embryonic Fibroblasts (MEFs) Using Adenovirus Expressing Cre Recombinase-arf-bp1$^{FL/Y}$—MEFs were prepared from E13.5 embryos and cultured in DMEM containing 10% FBS. To delete *arf-bp1*, 2.5×10^5 of cells were mixed with either control adenovirus expressing GFP (Ad-CMV-GFP; Vector Biolaboratories) or adenovirus expressing Cre (Ad-CMV-Cre; Vector Biolaboratories) at a multiplicity of infection of 200 before being plated onto a 6-well plate. Cells were harvested after 3 days, and protein extracts were prepared in radioimmunepreciptation assay buffer and analyzed by Western blotting. The Western blot was probed with antibodies against ARF-BP1 (Bethyl), p53 (CM5; Novocastra), p21 (Santa Cruz Biotechnology), BAX (Santa Cruz Biotechnology), and β-actin (Sigma).

RESULTS

Generation of arf-bp1 Conditional Knock-out Mice—The mouse *arf-bp1* gene is located on the X chromosome and contains 83 exons in a span of more than 100 kb of genomic DNA (Ensembl). Because of the location and the size of *arf-bp1*, we decided to create a conditional knock-out allele of *arf-bp1*, in which exon 11 is flanked by loxP sites (floxed) to permit deletion of exon 11 upon Cre expression (Fig. 1*A*). After gene targeting in mouse embryonic stem cells, 2 of 200 clones screened were identified to have correct homologous recombination events by Southern blotting. Subsequently, these clones were injected into mouse blastocysts to derive chimeras, from which germ line transmission of the targeted allele was accomplished. Subsequently, homozygote conditional knock-out males (*arf-bp1*$^{FL/Y}$) and females (*arf-bp1*$^{FL/FL}$) were obtained through breeding, which were grossly normal and fertile, suggesting that floxing exon 11 has no discernible effects on *arf-bp1* transcription.

arf-bp1 Knock-out Mice Were Embryonic Lethal—To understand the impacts of knock-out of *arf-bp1 in vivo*, we generated *arf-bp1* knock-out mice (*arf-bp1*$^{-/Y}$) through breeding between *arf-bp1*$^{FL/+}$ heterozygote conditional knock-out female mice and *Rosa26-cre* homozygote male mice. Because of constitutive Cre expression from the *Rosa26-cre* allele, mice with the genotype of *arf-bp1*$^{FL/Y}$*/Rosa26-cre* were considered as *arf-bp1* knock-out mice (*arf-bp1*$^{-/Y}$). There were 47 wild-type offspring at weaning age (Table 1), and no *arf-bp1* homozygote knock-out mice were obtained postnatally (23 were expected), suggesting that *arf-bp1* knock-out mice were embryonic lethal. Furthermore, the number of *arf-bp1* heterozygote knock-out (*arf-bp1*$^{+/-}$) mice (8 were observed) was underrepresented (23 were expected), presumably due to random X chromosome inactivation of the remaining wild-type allele. To analyze the phenotypes of *arf-bp1* knock-out mice, embryos from E11.5 to E17.5 were collected, from which a*rf-*

TABLE 1
Analysis of offspring and embryos from the cross between *ARF-BP1*$^{FL/+}$ females with *Rosa26*$^{Cre/Cre}$ males

Stage (dpc)[a]	Genotype		
	+/+, +/Y	+/−	−/Y
Expected ratio	2	1	1
11.5	2	2	4
12.5	21(1)[b]	10	12
13.5	33(1)[b]	12	17
14.5	12	6	4[c]
16.5	18(1)[b]	4(1)[b]	8[c]
17.5	5	2(1)[b]	2[c]
Total embryos	91	36	47
Offspring	47	8	0

[a] Days postcoitus.
[b] The number of abnormal embryos is indicated in parentheses.
[c] All embryos had hemorrhage and were dead.

bp1 knock-out embryos were identified at all stages during development (Table 1). Although *arf-bp1* knock-out embryos at E12.5 (Fig. 2*D*) appeared indistinguishable from wild-type embryos (Fig. 2*A*), all of the *arf-bp1* knock-out embryos displayed hemorrhage in the abdominal region by E14.5 (Fig. 2*E*), followed by growth impairment, necrosis, and eventual death of the embryos (Fig. 2*F*). Age-matched control embryos are shown (Fig. 2, *B* and *C*). These results confirmed that *arf-bp1* knock-out mice were embryonic lethal during late stage of embryonic development.

Ablation of arf-bp1 in Mouse Resulted in p53 Activation—To explore the molecular mechanism for the embryonic lethality in *arf-bp1* knock-out mice, sagittal sections were prepared from the embryos collected at multiple stages from timed mating. The sections were immunostained using an anti-ARF-BP1 antibody (Bethyl), which recognizes the middle portion of ARF-BP1 protein. As expected, ARF-BP1 could be detected in nucleus and cytoplasm in the cells from wild-type embryos (Fig. 2*G*). In contrast, almost all of the cells in *arf-bp1* knock-out embryos had lost the staining of ARF-BP1 by E13.5, indicating sufficient depletion of ARF-BP1 protein in the cells from *arf-bp1* knock-out embryos (Fig. 2*J*). Because ARF-BP1 has been shown to regulate p53 stability (11), sections from *arf-bp1* knock-out embryos were immunostained using anti-p53 antibody (Novocastra). Indeed, staining of p53 was detected in neural cells at E13.5 (Fig. 2*K*), compared with those of the control embryos (Fig. 2*H*), demonstrating that ablation of ARF-BP1 resulted in accumulation of p53 protein. In addition, Cleaved Caspase3 staining was also readily detected in these cells in *arf-bp1* knock-out embryos (Fig. 2*L*) compared with those of the control embryos (Fig. 2*I*), suggesting that accumulation of p53 led to activation of apoptosis. Together, these data suggest that the embryonic lethality of *arf-bp1* knock-out mice was, at least, in part, due to p53 activation in the absence of functional ARF-BP1.

Ablation of ARF-BP1 in Pancreatic β-Cells in mice Resulted in Progressive Hyperglycemia and Development of Diabetes—Although the above data indeed validate the role of ARF-BP1 in p53 regulation *in vivo*, with very limited ARF-BP1-null cells/tissues, the physiological role of ARF-BP1 in p53 regulation could not be determined. The difficulty in studying these *arf-bp1* knock-out mice has amplified the importance of generating additional ARF-BP1 mutant mice in different organs to facilitate the analysis of the biological phenotypes in adult tissues.

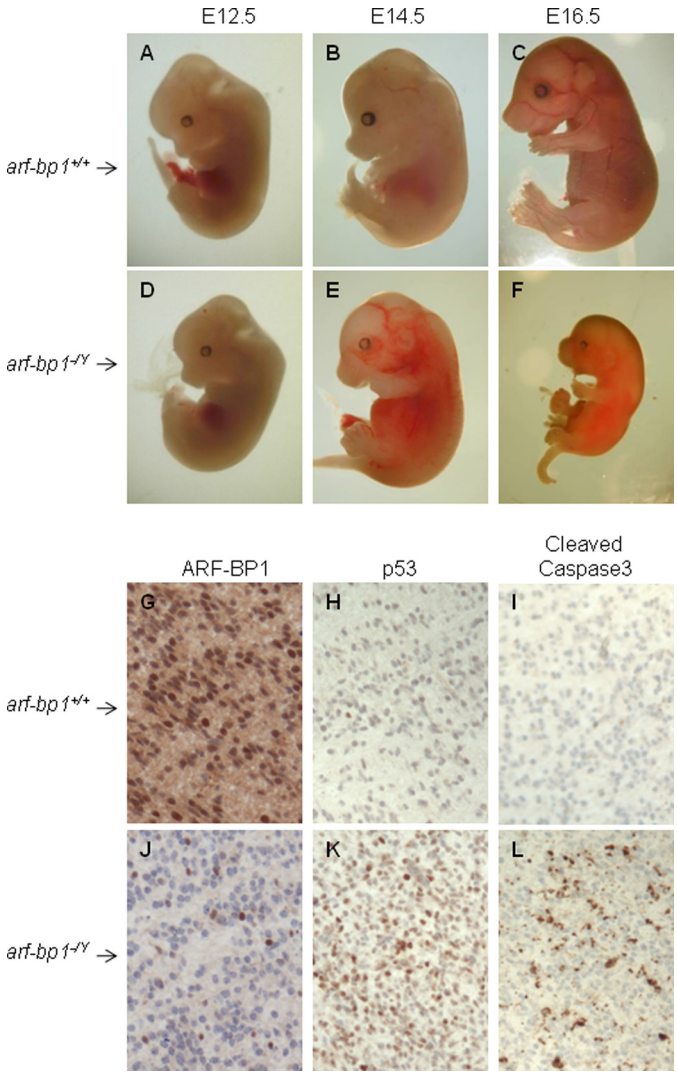

FIGURE 2. ***arf-bp1* knock-out mice were embryonic lethal and showed p53 activation.** *A–F*, representative wild-type embryos (*arf-bp1*$^{+/+}$) (*A–C*) and *arf-bp1* knock-out embryos (*arf-bp1*$^{-/Y}$) (*D–F*) from days E12.5, E14.5, and E16.5. *G–L*, sections of E13.5 embryos of wild-type embryos (*G–I*) and *arf-bp1* knock-out embryos (*J–L*) immunostained using antibodies against ARF-BP1 (*G* and *J*), p53 (*H* and *K*), and Cleaved Caspase3 (*I* and *L*).

We chose to delete *arf-bp1* in pancreatic β-cells because of the minimal effect on embryonic development by disruption of β-cell functions and the significant expression of ARF-BP1 in β-cells (Fig. 3*Ai*). Thus, we generated conditional *arf-bp1* mutant mice with specific deletion of *arf-bp1* in pancreatic β-cells, mediated by *RIP-cre* (24, 25). The *arf-bp1*$^{FL/Y}$/*RIP-cre* mice were born close to Mendelian ratio and appeared normal; in particular, they had similar body weight compared with the control mice at least up to 6 months of age (supplemental Fig. 1). To determine whether *arf-bp1* was efficiently ablated in β-cells, sections of pancreas from 1-month-old mice were immunostained using antibodies against ARF-BP1, insulin, and glucagon. ARF-BP1 staining was present in nucleus and cytoplasm of the β-cells of the control mice (Fig. 3*Ai*). Some of the β-cells showed no staining of ARF-BP1, presumably due to lack of expression of ARF-BP1 in proliferating cells, as observed previously (26). This is consistent with the fact that *arf-bp1* conventional knock-out embryos died at late gestation stage

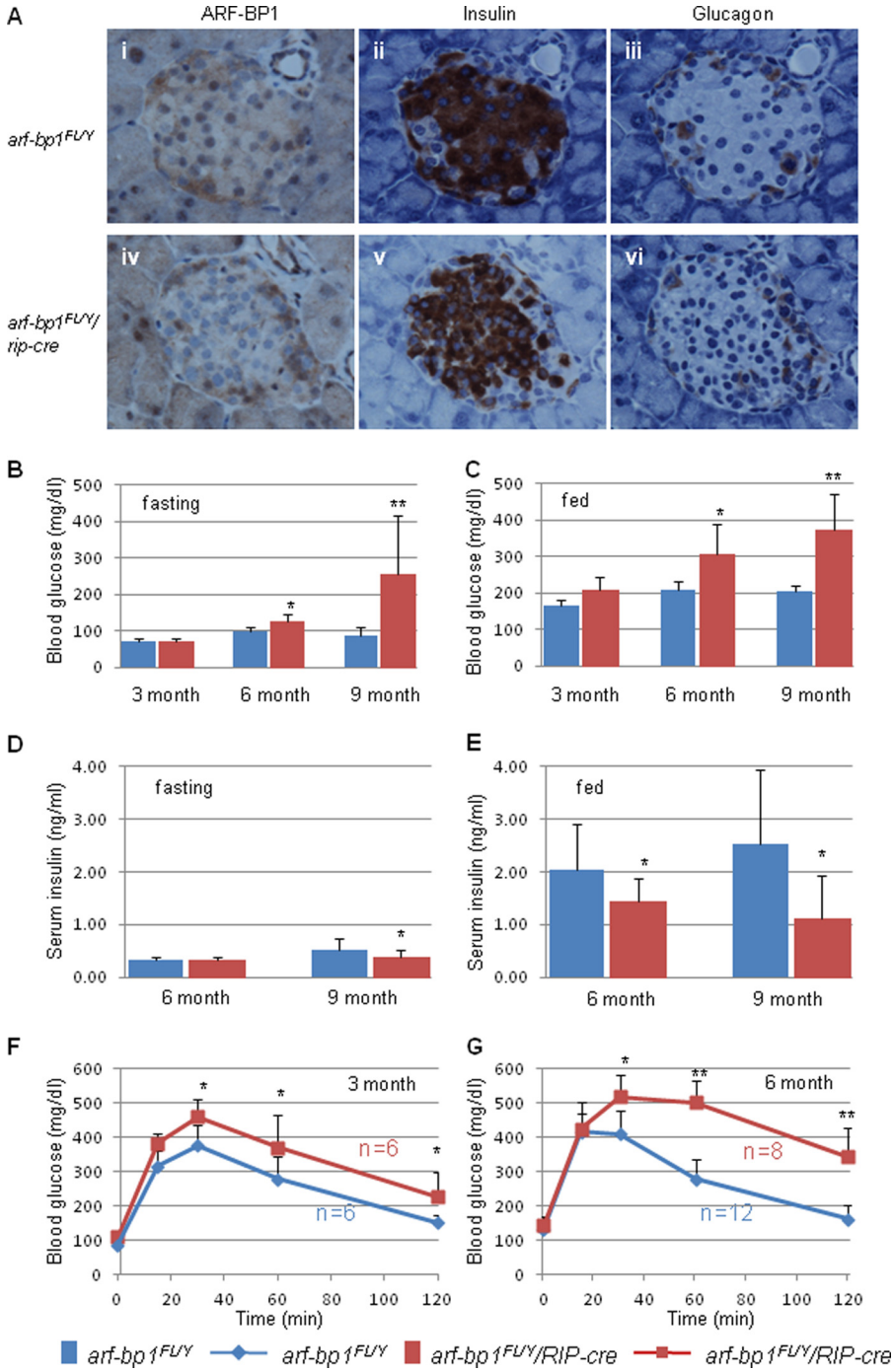

FIGURE 3. **Conditional Knock-out mice of *arf-bp1* in pancreatic β-cells developed hyperglycemia progressively.** *A*, pancreases from 1-month-old control mice (*arf-bp1*$^{FL/Y}$) (*i–iii*) and *arf-bp1*$^{FL/Y}$/*RIP-cre* mice (*iv–vi*) were immunostained using antibodies against ARF-BP1 (*i* and *iv*), insulin (*ii* and *v*), and glucagon (*iii* and *vi*). *B* and *C*, fasting (*B*) and fed (*C*) blood glucose levels were determined for control mice (*blue bars*) and *arf-bp1*$^{FL/Y}$/*RIP-cre* mice (*red bars*) 3, 6, and 9 months old. *D* and *E*, fasting (*D*) and fed (*E*) blood insulin levels were determined for 6- and 9-month-old mice. *F* and *G*, GTT was performed on *arf-bp1*$^{FL/Y}$/*RIP-cre* mice (*red lines*) and control mice (*blue lines*) using 3-month-old (*F*) and 6-month-old (*G*) mice. Data are presented as mean ± S.D. (*error bars*). Statistical significance was assessed using Student's *t* test (*, $p < 0.05$; **, $p < 0.001$).

(E14.5), indicating critical functions of ARF-BP1 in postmitotic cells. In contrast, there was no staining for ARF-BP1 in the β-cells in the islets of *arf-bp1*$^{FL/Y}$/*RIP-cre* mice (Fig. 3*Aiv*), demonstrating that ARF-BP1 was sufficiently depleted in the β-cells due to *RIP-cre*-mediated *arf-bp1* deletion. Consistent with the specificity of the *RIP-cre* expression, there was no difference of ARF-BP1 staining in the α-cells of the islets and the surrounding acinar cells of the pancreas between *arf-bp1*$^{FL/Y}$/*RIP-cre* mice and the control mice (Fig. 3*A*, *iv versus i*). Interestingly, there was a similar staining for insulin in the β-cells (located in the core of the islet) (Fig. 3*Av*) in the absence of ARF-BP1 in *arf-bp1*$^{FL/Y}$/*RIP-cre* mice compared with that of the control mice (Fig. 3*Aii*). There was no significant difference for glucagon staining (located in the periphery of the islet) between the control and the *arf-bp1*$^{FL/Y}$/*RIP-cre* mice (Fig. 3*A*, *iii versus vi*).

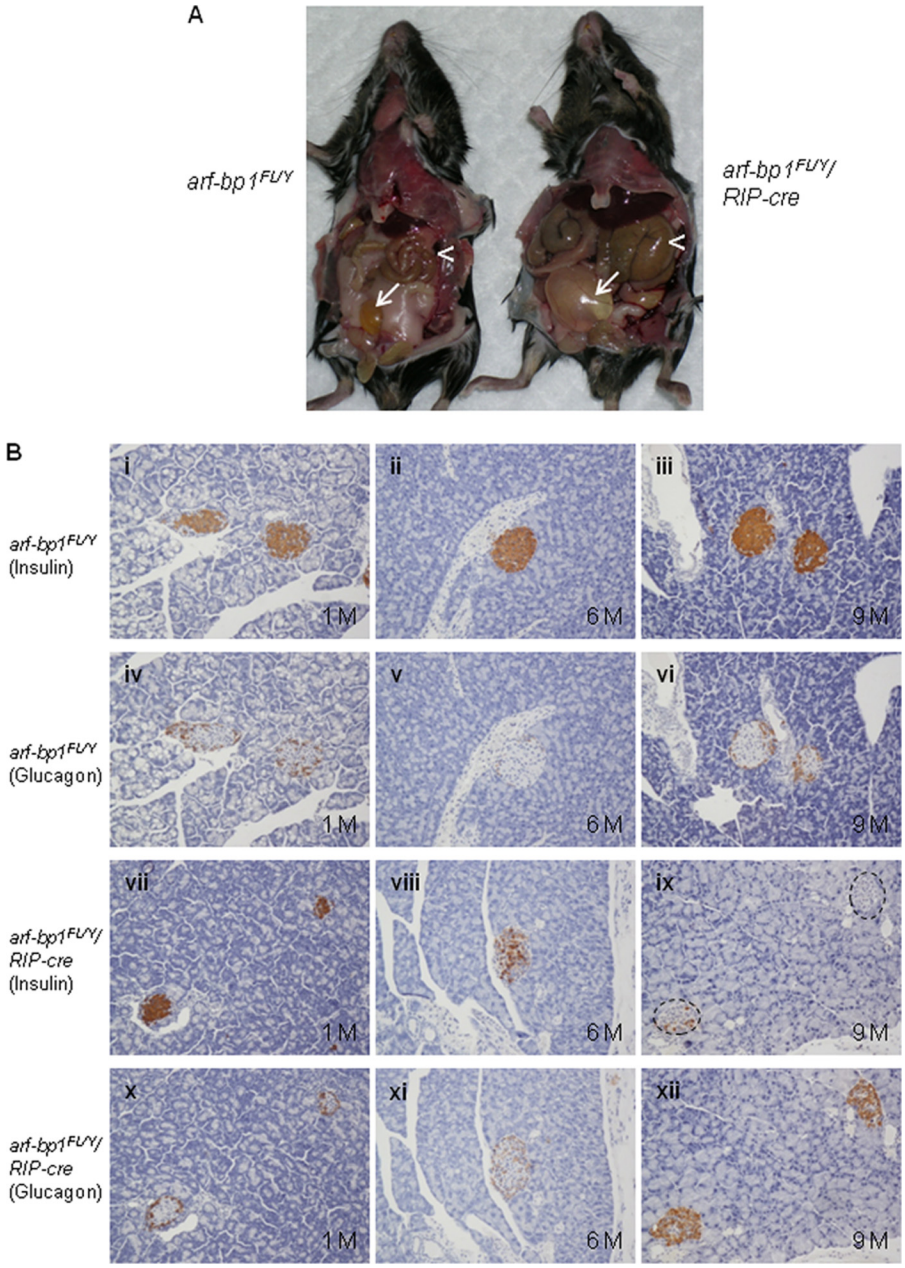

FIGURE 4. **Loss of pancreatic β-cells in aged *arf-bp1*$^{FL/Y}$*/RIP-cre* mice.** *A*, representative 9-month-old control mouse (*left*) and *arf-bp1*$^{FL/Y}$*/RIP-cre* mouse (*right*). *Arrows* indicate the bladders in the control and *arf-bp1*$^{FL/Y}$*/RIP-cre* mice, and *arrowheads* indicate intestine in the control and *arf-bp1*$^{FL/Y}$*/RIP-cre* mice. *B*, immunostaining of pancreases from the control (*i–vi*) and from the *arf-bp1*$^{FL/Y}$*/RIP-cre* mice (*vii–xii*). *i*, *iv*, *vii*, and *x*, 1-month-old mice; *ii*, *v*, *viii*, and *xi*, 6-month-old mice; and *iii*, *vi*, *ix*, and *xii*, 9-month-old mice. Antibodies against insulin (*i–iii* and *vii–ix*) and glucagon (*iv–vi* and *x–xii*) were used. *Dotted circles* in *ix* outline the islets.

To determine the long term effects of *arf-bp1* deletion on the β-cell functions, the blood glucose was monitored periodically. In addition, the proficiency of insulin response was determined by GTT at 3 and 6 months of age. Consistent with the insulin staining in islets from young mice, both fasting and fed glucose levels of *arf-bp1*$^{FL/Y}$*/RIP-cre* mice showed similar levels during the first 2 months, compared with those of the control *arf-bp1*$^{FL/Y}$ mice (Fig. 3, *B* and *C*). However, as *arf-bp1*$^{FL/Y}$*/RIP-cre* mice aged, blood glucose levels became increasingly higher than those of the control mice (Fig. 3, *B* and *C*). For the fed blood glucose levels (Fig. 3*C*), in particular, the average fed blood glucose level was 209 mg/dl for *arf-bp1*$^{FL/Y}$*/RIP-cre* mice *versus* 167 mg/dl for the control mice at 3 months old; the differences increased to 308 *versus* 208 mg/dl at 6 months old and 373 *versus* 204 mg/dl at 9 months old (Fig. 3*C*). Consistently, fed insulin levels were decreased significantly in *arf-bp1*$^{FL/Y}$*/RIP-cre* mice at 6 and 9 months old of age compared with those of the control mice (Fig. 3*E*). There were also significant lower fasting insulin levels for *arf-bp1*$^{FL/Y}$*/RIP-cre* mice than the control mice at 9 months old (Fig. 3*D*). Furthermore, the insulin deficiency was confirmed by GTT. As shown in Fig. 3*F*, the glucose levels were significantly higher along the time course after glucose injection in *arf-bp1*$^{FL/Y}$*/RIP-cre* mice than those of the control mice at 3

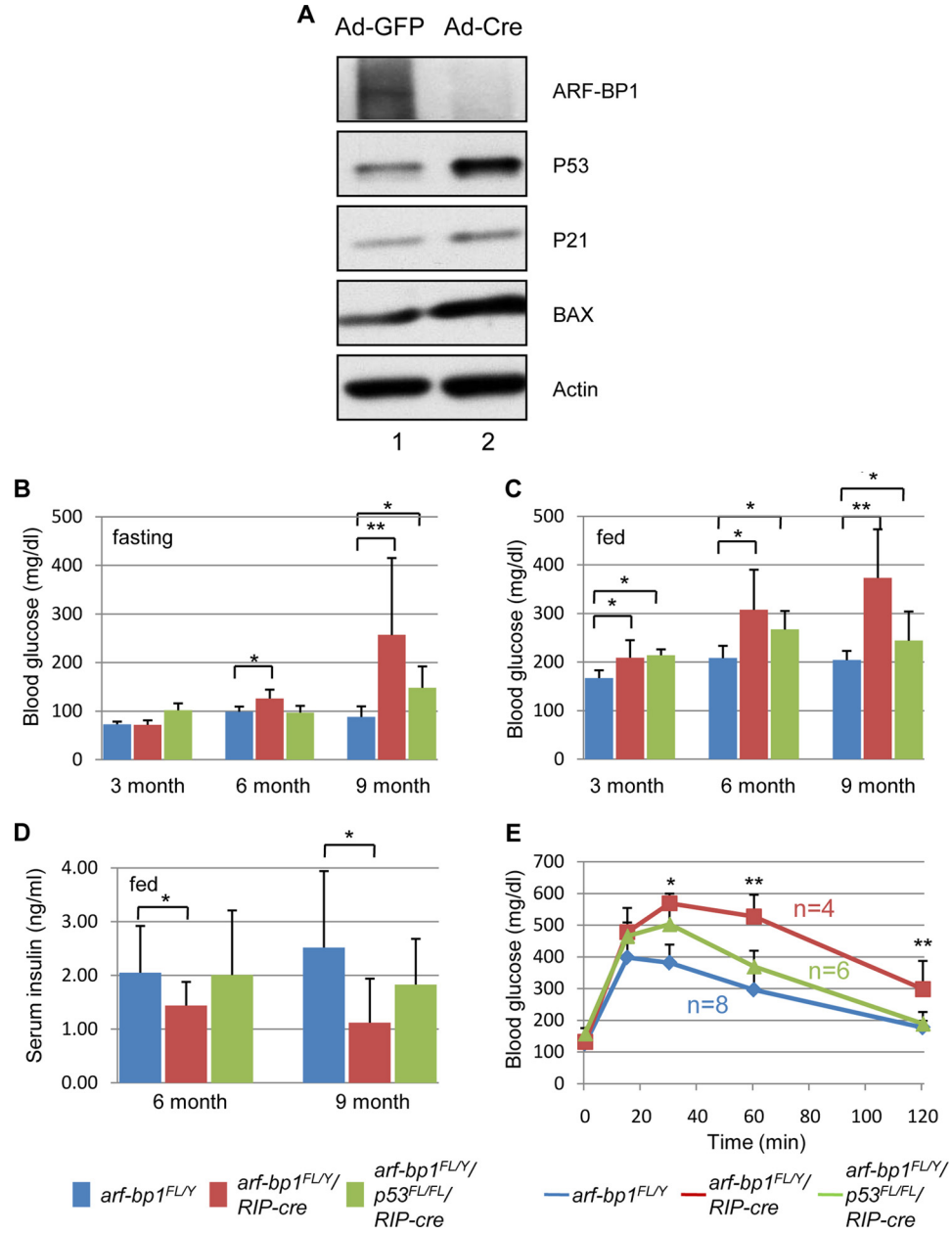

FIGURE 5. **Partial rescue of the hyperglycemia condition in *arf-bp1*$^{FL/Y}$*/RIP-cre* mice by concomitant deletion of *p53*.** *A*, Western blot of the whole cell extracts from *arf-bp1*$^{FL/Y}$ MEFs infected with control adenovirus Ad-GFP (*lane 1*) or with Ad-Cre (*lane 2*) using antibodies against ARF-BP1, p53, p21, BAX, and β-actin. *B* and *C*, fasting (*B*), and fed (*C*) blood glucose levels determined for control mice (*blue bars*), *rf-bp1*$^{FL/Y}$*/RIP-cre* mice (*red bars*), and *arf-bp1*$^{FL/Y}$*/p53*$^{FL/FL}$*/RIP-cre* mice (*green bars*) 3, 6, and 9 months old. *D*, fed blood insulin levels determined for control mice (*blue bars*), *arf-bp1*$^{FL/Y}$*/RIP-cre* mice (*red bars*), and *arf-bp1*$^{FL/Y}$*/p53*$^{FL/FL}$*/RIP-cre* mice (*green bars*) 6 and 9 months of age. *E*, GTT for control mice (*blue line*), *arf-bp1*$^{FL/Y}$*/RIP-cre* mice (*red line*), and *arf-bp1*$^{FL/Y}$*/p53*$^{FL/FL}$*/RIP-cre* mice (*green line*) 6 months of age. Data are presented as mean ± S.D. (*error bars*). Statistical significance was assessed using Student's *t* test (*, $p < 0.05$; **, $p < 0.001$).

months old. The differences in GTT became even bigger for 6-month-old mice, suggesting further decline of insulin response in aged *arf-bp1*$^{FL/Y}$*/RIP-cre* mice (Fig. 3*G*). Moreover, many of the *arf-bp1*$^{FL/Y}$*/RIP-cre* mice (Fig. 4*A*, *right*) displayed typical signs for diabetes, such as excessive urination due to high blood glucose, and upon dissection, greatly enlarged bladder (Fig. 4*A*, *arrows*), and excess food in the intestine (Fig. 4*A*, *arrowheads*). Many of the mice had fed blood glucose levels higher than 600 mg/dl (limit of the glucometer). More than half of the mice died at <1 year of age, due to severe diabetic symptoms (see Fig. 6*A*, *red line*).

Insulin Deficiency in arf-bp1$^{FL/Y}$*/RIP-cre Mice Was Caused by Loss of Pancreatic β-Cells*—To determine the cause of the hyperglycemia and insulin deficiency, sections of pancreas from *arf-bp1*$^{FL/Y}$*/RIP-cre* mice were collected and immunostained for insulin (β-cells) and glucagon (α-cells). At 1 month old, the islets from *arf-bp1*$^{FL/Y}$*/RIP-cre* mice had normal appearances of round shape, with center-located β-cells and periphery-located α-cells (Fig. 4*B*, *vii* and *x versus i* and *iv*, respectively). At 6 months old, the morphology of islets in *arf-bp1*$^{FL/Y}$*/RIP-cre* mice became increasingly irregular with frequent infiltration of α-cells in the middle of the islets (Fig. 4*B*,

viii and *xi versus ii* and *v*, respectively). Disruption of the islet structure was worsened in aged mice of >9 months old, in which there was near absence of insulin staining in the islets from *arf-bp1*$^{FL/Y}$/*RIP-cre* mice (Fig. 4*B*, *ix versus iii*), suggesting dramatic loss of β-cells as mice aged. The remaining cells in the islets were α-cells because they were positive for glucagon staining (Fig. 4*B*, *xii versus vi*).

Diabetic Conditions of arf-bp1$^{FL/Y}$*; RIP-cre mice Were Significantly Rescued by Concomitant p53 Ablation*—Our previous study showed that ARF-BP1 plays an important role in down-regulation of p53 because RNAi-mediated knockdown of ARF-BP1 increases the basal levels (~3-fold) of p53 proteins and enhances p53-mediated functions in human cell lines (11). Thus, it is very likely that the cause for the aging-dependent decrease of β-cell population in *arf-bp1*$^{FL/Y}$/*RIP-cre* mice is the high basal levels of p53 in these ARF-BP1-depleted β-cells and that these cells are more sensitive to normal physiological stress. To confirm the role of ARF-BP1 in regulating p53 function, we decided to delete *arf-bp1* in *arf-bp1*$^{FL/Y}$ MEFs infected with Cre-expressing adenovirus (Ad-cre), which allowed detailed analysis of the effects on p53 function by *arf-bp1* inactivation. As shown in Fig. 5*A*, whereas ARF-BP1 was expressed as a protein of about 500 kDa in wild-type cells (*lane 1*), no ARF-BP1 protein was detected in *arf-bp1*$^{FL/Y}$ cells after Ad-cre virus infection (Fig. 5*A*, *lane 2*), demonstrating depletion of ARF-BP1 protein after deletion of *arf-bp1*. Significantly, p53 was accumulated in *arf-bp1* knock-out cells, which led to activation of its targets p21 and apoptotic gene *BAX* (Fig. 5*A*, *lane 2 versus lane 1*). These results showed that deletion of *arf-bp1* indeed led to stabilization and activation of p53.

To determine further whether loss of β-cells in *arf-bp1*$^{FL/Y}$/*RIP-cre* mice was due to activation of p53 under physiological settings, we generated *arf-bp1*$^{FL/Y}$/*p53*$^{FL/FL}$/*RIP-cre* double knock-out mice, in which both *arf-bp1* and *p53* were deleted in β-cells. Dramatically, the hyperglycemia conditions in *arf-bp1*$^{FL/Y}$/*RIP-cre* mice were alleviated in *arf-bp1*$^{FL/Y}$/*p53*$^{FL/FL}$/*RIP-cre* mice. Both fasting (Fig. 5*B*, *green bar*) and fed (Fig. 5*C*, *green bar*) blood glucose levels were lowered in *arf-bp1*$^{FL/Y}$/*p53* $^{FL/FL}$/*RIP-cre* mice compared with those of the *arf-bp1*$^{FL/Y}$/*RIP-cre* mice (Fig. 5, *B* and *C*, *red bar*). Consistently, insulin levels in *arf-bp1*$^{FL/Y}$/*p53*$^{FL/FL}$/*RIP-cre* mice (Fig. 5*D*, *green bar*) were higher than that of *arf-bp1*$^{FL/Y}$/*RIP-cre* mice (Fig. 5*D*, *red bar*). Furthermore, GTT using 6-month-old mice revealed significant improvement of insulin response in *arf-bp1*$^{FL/Y}$/*p53*$^{FL/FL}$/*RIP-cre* mice (Fig. 5*E*, *green line*), as the glucose level at the end of the assay for *arf-bp1*$^{FL/Y}$/*p53* $^{FL/FL}$/*RIP-cre* mice was nearly the same as that of the control mice (Fig. 5*E*, *green line versus blue line*). In contrast, the glucose levels for *arf-bp1*$^{FL/Y}$/*RIP-cre* mice were significantly higher than that of the control mice at the end of the assay (Fig. 5*E*, *red line*). Notably, the double knock-out mice survived much longer than the *arf-bp1*$^{FL/Y}$/*RIP-cre* mice, due to overall improvement of the diabetic condition (Fig. 6*A*, *green line*).

Furthermore, histology analysis of pancreases revealed similar architecture of islets and the abundance of β-cells in *arf-bp1*$^{FL/Y}$/*p53*$^{FL/FL}$/*RIP-cre* mice (Fig. 6*H*) compared with the *arf-bp1*$^{FL/Y}$/*p53*$^{FL/FL}$ 9-month-old mice (Fig. 6*F*), whereas the α-cells maintained their peripheral localization (Fig. 6, *I versus G*). These histological features represented significant improvement of *arf-bp1*$^{FL/Y}$/*p53*$^{FL/FL}$/*RIP-cre* mice compared with *arf-bp1*$^{FL/Y}$/*RIP-cre* mice, which showed dramatic reduction of insulin staining and disorganized islets (Fig. 6, *D* and *E*). Insulin and glucagon staining of 9-month-old *arf-bp1*$^{FL/Y}$ mice was included for comparison (Fig. 6, *B* and *C*, respectively). Together, these results suggested that the diabetic phenotype in *arf-bp1*$^{FL/Y}$/*RIP-cre* mice was significantly rescued by *p53* gene ablation.

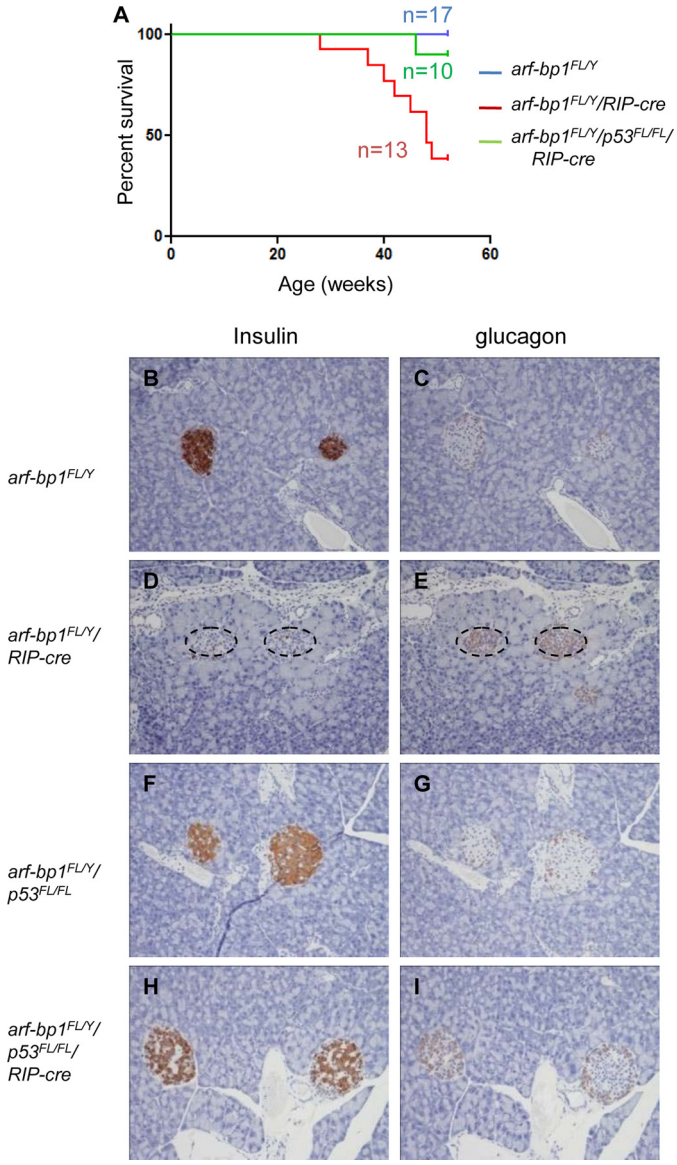

FIGURE 6. **Life span extension and improvement of islet histology in *arf-bp1/p53/RIP-cre* double knock-out mice.** *A*, percentage of survival for the control mice (*blue line*), *arf-bp1*$^{FL/Y}$/*RIP-cre* mice (*red line*), and *arf-bp1*$^{FL/Y}$/*p53*$^{FL/FL}$/*RIP-cre* mice (*green line*) during first year. B–I, immunostaining for insulin (*B*, *D*, *F*, and *H*) and immunostaining for glucagon (*C*, *E*, *G*, and *I*) using pancreas from 9-month-old control mice (*arf-bp1*$^{FL/Y}$/*p53*$^{FL/FL}$) (*F* and *G*) and *arf-bp1* $^{FL/Y}$/*p53* $^{FL/FL}$/*RIP-cre* mice (*H* and *I*) as well as pancreas from 9-month-old control mice (*arf-bp1*$^{FL/Y}$) (*B* and *C*) and *arf-bp1*$^{FL/Y}$/*RIP-cre* mice (*D* and *E*) for comparison. *Dotted circles* in *D* and *E* outline the islets.

DISCUSSION

This study demonstrated that *arf-bp1*$^{FL/Y}$/*RIP-cre* mice developed an age-dependent diabetic phenotype, due to loss of

β-cells. Evidence suggested that activation of p53 caused reduction of β-cell population in *arf-bp1*$^{FL/Y}$/*RIP-cre* mice, as concomitant knock-out of p53 significantly restored β-cell population and rescued the diabetic phenotype in *arf-bp1*$^{FL/Y}$/*RIP-cre* mice. These finding are consistent with the function of ARF-BP1 in ubiquitination and stability of p53, which is also validated by the study of *arf-bp1* knock-out embryos and *arf-bp1* knock-out MEFs. Interestingly, recent studies revealed that up-regulation of p53 contributes to β-cell apoptosis and diabetes, highlighting the importance of controlling p53 activation in β-cells (27–30). In addition, several studies have shown an age-dependent decline of β-cell regeneration and functions, due to increase of expression of ARF (31–33). It is intriguing whether ARF regulates β-cell functions through its ability to inhibit ARF-BP1. Although several E3 ubiquitin ligases have been identified to regulate p53 (34, 35), ARF-BP1 is the first E3 ubiquitin ligase of p53, other than Mdm2, shown to regulate p53 functions under physiological settings. Moreover, although our results demonstrate that p53 is regulated by ARF-BP1 *in vivo*, deregulation of other substrates of ARF-BP1 may also contribute to the phenotype of ARF-BP1 mutant mice, which clearly needs further elucidation in the future.

The p53 protein is well established as a major tumor suppressor in almost every type of human cancers because of its crucial functions in coordinating cellular responses to genotoxic stress and its irreplaceable roles in suppressing tumorigenesis. p53 is a short lived protein whose activity is maintained at low levels by both Mdm2-dependent and Mdm2-independent mechanisms in normal cells. The cellular functions of p53 are rapidly activated in response to stress, and tight regulation of p53 is essential for its effect on tumorigenesis as well as maintaining normal cell growth. Importantly, restoration of p53 activity remains an important goal in the quest for more effective cancer therapeutics. Indeed, Nutlin-3, a small molecule inhibitor of Mdm2, is able to activate p53 and exhibits antitumor efficacy in cancer cells that express wild-type p53 (36). Notably, in some cases the activity of p53 can be dangerous for the organism. Thus, p53-dependent apoptosis induced in normal tissues during chemo- and radiotherapy can cause severe side effects of antitumor therapy and, therefore, limits its efficiency. Our study showed that p53 activation in *arf-bp1* mutant mice is the major cause of severe diabetic symptoms and shortened life span. More importantly, the diabetic phenotype of these mice was largely reversed by p53 ablation, and the life span of the mice was also extended. Further studies are required to examine whether p53 is indeed overactivated in diabetic patients. If so, it will be interesting to test whether pifithrin-α, a previously indentified small molecule inhibitor of p53 (37, 38), is beneficial in the treatment of diabetes. In this regard, it is also interesting to know whether small molecule activators of SirT1, a deacetylase of p53 (39, 40), can improve glucose homeostasis and insulin sensitivity, partially through modulating p53 function.

REFERENCES

1. Zhang, Y., and Lu, H. (2009) Signaling to p53: ribosomal proteins find their way. *Cancer Cell* **16,** 369–377
2. Kruse, J. P., and Gu, W. (2009) Modes of p53 regulation. *Cell* **137,** 609–622
3. Vousden, K. H., and Prives, C. (2009) Blinded by the light: the growing complexity of p53. *Cell* **137,** 413–431
4. Qian, Y., and Chen, X. (2010) Tumor suppression by p53: making cells senescent. *Histol. Histopathol.* **25,** 515–526
5. Marine, J. C., and Lozano, G. (2010) Mdm2-mediated ubiquitylation: p53 and beyond. *Cell Death Differ,* **17,** 93–102
6. Jones, S. N., Roe, A. E., Donehower, L. A., and Bradley, A. (1995) Rescue of embryonic lethality in Mdm2-deficient mice by absence of p53. *Nature* **378,** 206–208
7. Montes de Oca Luna, R., Wagner, D. S., and Lozano, G. (1995) Rescue of early embryonic lethality in mdm2-deficient mice by deletion of p53. *Nature* **378,** 203–206
8. Ringshausen, I., O'Shea, C. C., Finch, A. J., Swigart, L. B., and Evan, G. I. (2006) Mdm2 is critically and continuously required to suppress lethal p53 activity *in vivo*. *Cancer Cell* **10,** 501–514
9. Dornan, D., Wertz, I., Shimizu, H., Arnott, D., Frantz, G. D., Dowd, P., O'Rourke, K., Koeppen, H., and Dixit, V. M. (2004) The ubiquitin ligase COP1 is a critical negative regulator of p53. *Nature* **429,** 86–92
10. Leng, R. P., Lin, Y., Ma, W., Wu, H., Lemmers, B., Chung, S., Parant, J. M., Lozano, G., Hakem, R., and Benchimol, S. (2003) Pirh2, a p53-induced ubiquitin-protein ligase, promotes p53 degradation. *Cell* **112,** 779–791
11. Chen, D., Kon, N., Li, M., Zhang, W., Qin, J., and Gu, W. (2005) ARF-BP1/Mule is a critical mediator of the ARF tumor suppressor. *Cell* **121,** 1071–1083
12. Zhang, X., Berger, F. G., Yang, J., and Lu, X. (2011) USP4 inhibits p53 through deubiquitinating and stabilizing ARF-BP1. *EMBO J.* **30,** 2177–2189
13. Eischen, C. M., and Lozano, G. (2009) p53 and MDM2: antagonists or partners in crime? *Cancer Cell* **15,** 161–162
14. Zhang, Y. (2004) The ARF-B23 connection: implications for growth control and cancer treatment. *Cell Cycle* **3,** 259–262
15. Sherr, C. J. (2006) Divorcing ARF and p53: an unsettled case. *Nat. Rev. Cancer* **6,** 663–673
16. Herold, S., Hock, A., Herkert, B., Berns, K., Mullenders, J., Beijersbergen, R., Bernards, R., and Eilers, M. (2008) Miz1 and HectH9 regulate the stability of the checkpoint protein, TopBP1. *EMBO J.* **27,** 2851–2861
17. Zhong, Q., Gao, W., Du, F., and Wang, X. (2005) Mule/ARF-BP1, a BH3-only E3 ubiquitin ligase, catalyzes the polyubiquitination of Mcl-1 and regulates apoptosis. *Cell* **121,** 1085–1095
18. Zhao, X., Heng, J. I., Guardavaccaro, D., Jiang, R., Pagano, M., Guillemot, F., Iavarone, A., and Lasorella, A. (2008) The HECT-domain ubiquitin ligase Huwe1 controls neural differentiation and proliferation by destabilizing the *N*-Myc oncoprotein. *Nat. Cell Biol.* **10,** 643–653
19. Hall, J. R., Kow, E., Nevis, K. R., Lu, C. K., Luce, K. S., Zhong, Q., and Cook, J. G. (2007) Cdc6 stability is regulated by the Huwe1 ubiquitin ligase after DNA damage. *Mol. Biol. Cell* **18,** 3340–3350
20. Yin, L., Joshi, S., Wu, N., Tong, X., and Lazar, M. A. (2010) E3 ligases Arf-bp1 and Pam mediate lithium-stimulated degradation of the circadian heme receptor Rev-erbα. *Proc. Natl. Acad. Sci. U.S.A.* **107,** 11614–11619
21. Liu, Z., Miao, D., Xia, Q., Hermo, L., and Wing, S. S. (2007) Regulated expression of the ubiquitin protein ligase, E3(histone)/LASU1/Mule/ARF-BP1/HUWE1, during spermatogenesis. *Dev. Dyn.* **236,** 2889–2898
22. Liu, P., Jenkins, N. A., and Copeland, N. G. (2003) A highly efficient recombineering-based method for generating conditional knockout mutations. *Genome Res.* **13,** 476–484
23. Chen, Z., Trotman, L. C., Shaffer, D., Lin, H. K., Dotan, Z. A., Niki, M., Koutcher, J. A., Scher, H. I., Ludwig, T., Gerald, W., Cordon-Cardo, C., and Pandolfi, P. P. (2005) Crucial role of p53-dependent cellular senescence in suppression of Pten-deficient tumorigenesis. *Nature* **436,** 725–730
24. Herrera, P. L. (2000) Adult insulin- and glucagon-producing cells differentiate from two independent cell lineages. *Development* **127,** 2317–2322
25. Xuan, S., Kitamura, T., Nakae, J., Politi, K., Kido, Y., Fisher, P. E., Morroni, M., Cinti, S., White, M. F., Herrera, P. L., Accili, D., and Efstratiadis, A. (2002) Defective insulin secretion in pancreatic β-cells lacking type 1 IGF receptor. *J. Clin. Invest.* **110,** 1011–1019
26. Zhao, X., D'Arca, D., Lim, W. K., Brahmachary, M., Carro, M. S., Ludwig, T., Cardo, C. C., Guillemot, F., Aldape, K., Califano, A., Iavarone, A., and Lasorella, A. (2009) The N-Myc-DLL3 cascade is suppressed by the ubiq-

uitin ligase Huwe1 to inhibit proliferation and promote neurogenesis in the developing brain. *Dev Cell* **17,** 210–221
27. Gurzov, E. N., Germano, C. M., Cunha, D. A., Ortis, F., Vanderwinden, J. M., Marchetti, P., Zhang, L., and Eizirik, D. L. (2010) p53 up-regulated modulator of apoptosis (PUMA) activation contributes to pancreatic β-cell apoptosis induced by proinflammatory cytokines and endoplasmic reticulum stress. *J. Biol. Chem.* **285,** 19910–19920
28. Armata, H. L., Golebiowski, D., Jung, D. Y., Ko, H. J., Kim, J. K., and Sluss, H. K. (2010) Requirement of the ATM/p53 tumor suppressor pathway for glucose homeostasis. *Mol. Cell. Biol.* **30,** 5787–5794
29. Hinault, C., Kawamori, D., Liew, C. W., Maier, B., Hu, J., Keller, S. R., Mirmira, R. G., Scrable, H., and Kulkarni, R. N. (2011) Δ40 Isoform of p53 controls β-cell proliferation and glucose homeostasis in mice. *Diabetes* **60,** 1210–1222
30. Bitti, M. L., Saccucci, P., Capasso, F., Piccinini, S., Angelini, F., Rapini, N., Porcari, M., Arcano, S., Petrelli, A., Del Duca, E., Bottini, E., and Gloria-Bottini, F. (2011) Genotypes of p53 codon 72 correlate with age at onset of type 1 diabetes in a sex-specific manner. *J. Pediatr. Endocrinol. Metab.* **24,** 437–439
31. Chen, H., Gu, X., Su, I. H., Bottino, R., Contreras, J. L., Tarakhovsky, A., and Kim, S. K. (2009) Polycomb protein Ezh2 regulates pancreatic β-cell Ink4a/Arf expression and regeneration in diabetes mellitus. *Genes Dev.* **23,** 975–985
32. Krishnamurthy, J., Ramsey, M. R., Ligon, K. L., Torrice, C., Koh, A., Bonner-Weir, S., and Sharpless, N. E. (2006) p16INK4a induces an age-dependent decline in islet regenerative potential. *Nature* **443,** 453–457
33. Tschen, S. I., Dhawan, S., Gurlo, T., and Bhushan, A. (2009) Age-dependent decline in β-cell proliferation restricts the capacity of β-cell regeneration in mice. *Diabetes* **58,** 1312–1320
34. Migliorini, D., Bogaerts, S., Defever, D., Vyas, R., Denecker, G., Radaelli, E., Zwolinska, A., Depaepe, V., Hochepied, T., Skarnes, W. C., and Marine, J. C. (2011) Cop1 constitutively regulates c-Jun protein stability and functions as a tumor suppressor in mice. *J. Clin. Invest.* **121,** 1329–1343
35. Vitari, A. C., Leong, K. G., Newton, K., Yee, C., O'Rourke, K., Liu, J., Phu, L., Vij, R., Ferrando, R., Couto, S. S., Mohan, S., Pandita, A., Hongo, J. A., Arnott, D., Wertz, I. E., Gao, W. Q., French, D. M., and Dixit, V. M. (2011) COP1 is a tumor suppressor that causes degradation of ETS transcription factors. *Nature* **474,** 403–406
36. Vassilev, L. T., Vu, B. T., Graves, B., Carvajal, D., Podlaski, F., Filipovic, Z., Kong, N., Kammlott, U., Lukacs, C., Klein, C., Fotouhi, N., and Liu, E. A. (2004) *In vivo* activation of the p53 pathway by small-molecule antagonists of MDM2. *Science* **303,** 844–848
37. Komarov, P. G., Komarova, E. A., Kondratov, R. V., Christov-Tselkov, K., Coon, J. S., Chernov, M. V., and Gudkov, A. V. (1999) A chemical inhibitor of p53 that protects mice from the side effects of cancer therapy. *Science* **285,** 1733–1737
38. Gudkov, A. V., and Komarova, E. A. (2005) Prospective therapeutic applications of p53 inhibitors. *Biochem. Biophys. Res. Commun.* **331,** 726–736
39. Michan, S., and Sinclair, D. (2007) Sirtuins in mammals: insights into their biological function. *Biochem. J.* **404,** 1–13
40. Milne, J. C., Lambert, P. D., Schenk, S., Carney, D. P., Smith, J. J., Gagne, D. J., Jin, L., Boss, O., Perni, R. B., Vu, C. B., Bemis, J. E., Xie, R., Disch, J. S., Ng, P. Y., Nunes, J. J., Lynch, A. V., Yang, H., Galonek, H., Israelian, K., Choy, W., Iffland, A., Lavu, S., Medvedik, O., Sinclair, D. A., Olefsky, J. M., Jirousek, M. R., Elliott, P. J., and Westphal, C. H. (2007) Small molecule activators of SIRT1 as therapeutics for the treatment of type 2 diabetes. *Nature* **450,** 712–716